Photoluminescence of two-dimensional excitons in an electric field: Lifetime enhancement and field ionization in GaAs quantum wells

K. Köhler,* H.-J. Polland,† and L. Schultheis‡
Max-Planck-Institut für Festkörperforschung, 7000 Stuttgart 80, Federal Republic of Germany

C. W. Tu
AT&T Bell Laboratories, Murray Hill, New Jersey 07974
(Received 22 February 1988)

Two-dimensional excitons in GaAs/$Al_xGa_{1-x}As$ single quantum wells exposed to electric fields perpendicular to the layers are studied by means of time-resolved photoluminescence. The temporal decay of the excitonic emission distinguishes two characteristic field regimes: In the small-field regime, luminescence lifetime increases with increasing field, and a pronounced Stark shift is additionally observed. In the high-field domain ≥ 50 kV/cm, the lifetime decreases with increasing field because of excitonic field ionization, leading to carrier tunneling through the barriers. We discuss these features within the framework of a simple semiclassical model. Quantitative agreement is obtained for quantum wells of different well widths and barrier thicknesses with respect to lifetime, luminescence intensity, and tunneling current. Thus a consistent description of the dynamics of two-dimensional excitons exposed to an electric field is obtained.

I. INTRODUCTION

The photoluminescence properties of quantum wells (QW's) exposed to electric fields perpendicular to the layers significantly differ from the corresponding behavior of bulk GaAs.[1-5] Excitons in bulk GaAs ionize at fields below 4.5 kV/cm, as observed by the strong quenching of the photoluminescence (a considerable quenching is already observed at 700 V/cm), and exhibit only a small red shift of 0.2 meV.[6] In contrast, excitonic luminescence of quantum wells is even observable at electric fields up to 100 kV/cm and shifts towards lower energy as far as 90 meV.[1]

The optical properties of semiconductor QW's in an electric field have been extensively studied, both experimentally and theoretically.[1-5,7-28] A red shift of the transition energy observed in transmission has been attributed to the quantum-confined Stark effect (QCSE), i.e., polarization of electron-hole pairs within the wells.[8,9] A considerable shift towards lower energies in the QCSE regime was reported recently also for the photoluminescence.[1,2] In addition, an increase of the recombination lifetime was observed as a consequence of the decreased electron-hole overlap.[1]

However, for much higher electric fields tunneling of the carriers through the barriers must become important, which competes with the carrier recombination in the well and leads to strong quenching of the photoluminescence intensity.[9] In this field regime the new process leads simultaneously to a decrease of the total lifetime. It is the aim of this paper to emphasize the role of these two intrinsic processes in particular with respect to the QW width and barrier thickness. A simple model of QCSE *and* excitonic field ionization describes lifetime, Stark shift, and quenching quantitatively. Thus, a complete comprehensive understanding of the intrinsic electric-field-related spectral and temporal features of two-dimensional (2D) excitons in QW's is obtained.

Section II describes the samples investigated, the experimental methods, and the luminescence characterization. Electric-field effects in the regime of the QCSE are summarized in Sec. III. For field strengths up to ≈ 50 kV/cm a low-energy shift of the emission line and a corresponding increase of the recombination lifetime in broad QW's is found, both consistent with the field-induced charge separation and the corresponding decrease in electron-hole wave-function overlap. In Sec. IV A of the paper we will focus on our results of field ionization. For electric fields ≥ 50 kV/cm we observe a drastic decrease of both photoluminescence intensity and lifetime displaying the efficient tunneling of electrons and holes out of the well for *both* broad and thin QW's. Our experimental results are compared quantitatively with theoretical tunneling times, calculated in the model of the quasiclassical approximation. The subject of Sec. IV B is the influence of the barrier thickness on carrier tunneling. In Sec. IV C we compare the field dependence of the luminescence intensity and the tunneling current. A correlation is found between the photoluminescence lifetime and the decrease of the photoluminescence intensity in the regime of carrier tunneling. Section V concludes this work.

II. EXPERIMENTAL DETAILS AND OPTICAL CHARACTERIZATION

Our measurements are performed with two GaAs/$Al_{0.3}Ga_{0.7}As$ samples grown by molecular beam epitaxy on a Si-doped n^+ substrate. These samples contain single QW's with thicknesses of 5, 10.7, and 21.4 nm in sample no. 1 and 13.5 and 27.7 nm in sample no. 2. Barrier thicknesses between two adjacent wells are 24 and

14 nm for the respective samples. Thicknesses are evaluated from transmission electron microscopy measurements. The electric field is applied via a semitransparent Schottky contact which is formed by evaporating a guard ring structure with a 20-nm thick Au film onto the top of the $Al_xGa^{1-x}As$ cladding layer. The backside Ohmic contact is formed by alloying the n^+ substrate with indium. The samples are kept at low temperatures (5 K) for the measurements.

Time-resolved measurements on a picosecond time scale are performed by using picosecond pulses of a synchronously mode-locked continuous-wave (cw) dye laser pumped by an argon-ion laser. The pulse duration and the repetition rate are 3 ps and 80 MHz, respectively. The nanosecond experiments are carried out by single nanosecond pulses of 200-ns pulse duration and a repetition rate of 0.25 MHz generated by the emission of a tunable cw-dye laser and an acoustooptic modulator.

The photon energy of the exciting pulses on the sample is 1.66 eV, i.e., below the band gap of $Al_xGa_{1-x}As$. An excitation intensity between 10^{11} and 5×10^{12} photons/cm^2 per pulse is used which corresponds to peak carrier densities of 10^{15} and 5×10^{16} cm^{-3}, respectively. The time-resolved picosecond data are taken with a synchroscan streak camera and a 0.25-m monochromator giving a spectral and temporal resolution of 6 meV and 20 ps, respectively. Nanosecond experiments are performed with a gated photon counting system of variable pulse delay, connected to a 0.75-m monochromator. Here, the time resolution is 10 ns which is limited by the shape of the exciting pulse. The spectral resolution is 2 meV.

Time-integrated and cw-photoluminescence spectra are detected by a single grating monochromator with a nonintensified optical multichannel analyzer. The photodiode array is cooled down to -40 °C. The spectral resolution for these measurements is 0.1 meV. Results of the cw experiments are identical with the time-integrated measurements.

Luminescence spectra of the two samples taken under cw excitation are shown in Fig. 1. The measurements are taken under open circuit conditions, i.e., the photocurrent is practically zero. Five sets of luminescence lines are attributed to the QW's of 21.4, 10.7 and 5 nm in sample no. 1, respectively, and 27.7 and 13.5 nm in sample no. 2. The arrows indicate the heavy-hole (hh) exciton transition energy as observed in transmission or in photoluminescence excitation spectra. Emission of the light-hole (lh) exciton is seen for the broadest QW of 27.7 nm (sample no. 2) due to an appreciable thermal occupation. Because of the broad background emission of the n^+-GaAs substrate and the lower thermal occupation, the lh exciton luminescence cannot be detected for the other QW's. The dips in the n^+-substrate luminescence at the high-energy side of the 21.4-nm QW, 10.7-nm QW (sample no. 1), and 13.5-nm QW (sample no. 2) is due to absorption by the lh exciton of the broad emission originating from the n^+ substrate. On the low-energy side, broad emission lines are observed for all QW's with an increased spacing from the hh excitons emission peak for decreased well width, which is assigned to recombination

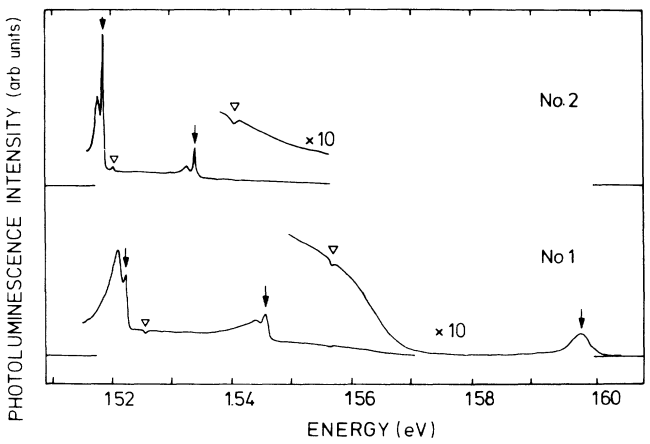

FIG. 1. Photoluminescence spectra of samples no. 1 (lower curve) and no. 2 (upper curve) at 5 K. The spectrum of sample no. 1 shows peaks attributed to the three QW's with thicknesses of 21.4, 10.7, and 5 nm, while in the upper spectrum of sample no. 2 two QW's with thicknesses of 27.7 and 13.5 nm are detected. Arrows indicate the hh exciton transition as observed in transmission respectively in excitation spectra. The triangles show the emission line of the lh exciton of the 27.7-nm QW (sample no. 2) and the absorption dip of the lh excitons of the 21.4-nm QW, 10.7-nm QW (sample no. 1) and the 13.5-nm QW (sample no. 2) in the broad emission of the n^+ substrate.

of excitons with donors and acceptors in analogy to the bulk case. In the case of the emission of the 5-nm QW (sample no. 1) the hh exciton transition is not clearly separated from bound exciton transitions involving donors. Absorption measurements in combination with the luminescence confirm these attributions.[29,7]

III. THE QCSE IN PHOTOLUMINESCENCE

Time-integrated photoluminescence spectra are also measured for different voltages applied between the GaAs n^+ substrate and the Au film. In spite of the drastic spectral line shift, the luminescence intensity does not change appreciably for voltages up to -2 V. Beyond this value a decrease of intensity is observed starting at different voltages for different QW's. Figure 2(a) shows the peak energy positions as a function of the external voltage V_{ext}. (At $V_{ext}\approx0.9V$ the built-in voltage is compensated and the photoluminescence corresponds to flat-band conditions.) The low-energy shift is much stronger for the thicker wells and reaches 90 meV for well thicknesses of 21.4 and 27.7 nm, whereas no significant shift is found for the 5-nm–thick well, as expected for the QCSE. The luminescence peak positions remain unaltered for the different excitation intensities used in our experiments.

The Schrödinger equation is numerically solved in the presence of an electric field for electrons and holes in a finite QW,[1] in order to quantitatively explain the shift by the QCSE. Effective electron and hole masses in the wells ($m_e=0.067m_0$, $m_h=0.34m_0$) and barriers ($m_e=0.092m_0$, $m_h=0.47m_0$) are taken from Miller *et al.*,[9] assuming a splitting of the discontinuity of the band gap between the conduction and valence band of 57:43. The

corresponding exciton binding energy is taken from Greene *et al.*[30] Fit parameters are avoided since the well thicknesses of our samples are accurately known. Figure 2(b) shows theoretical curves for the photoluminescence energy peak position as obtained by calculating the wave function and energy positions of electrons and heavy holes in a finite QW. Excellent agreement between experiment and theory is found for the absolute value and field dependence of the energy peak position, when we assume that a decrease of 1 V corresponds to an increase of the internal field strength of 15 kV/cm, leading to a one-to-one correspondence of voltage and electrical-field axis in Fig. 2(a) and 2(b).

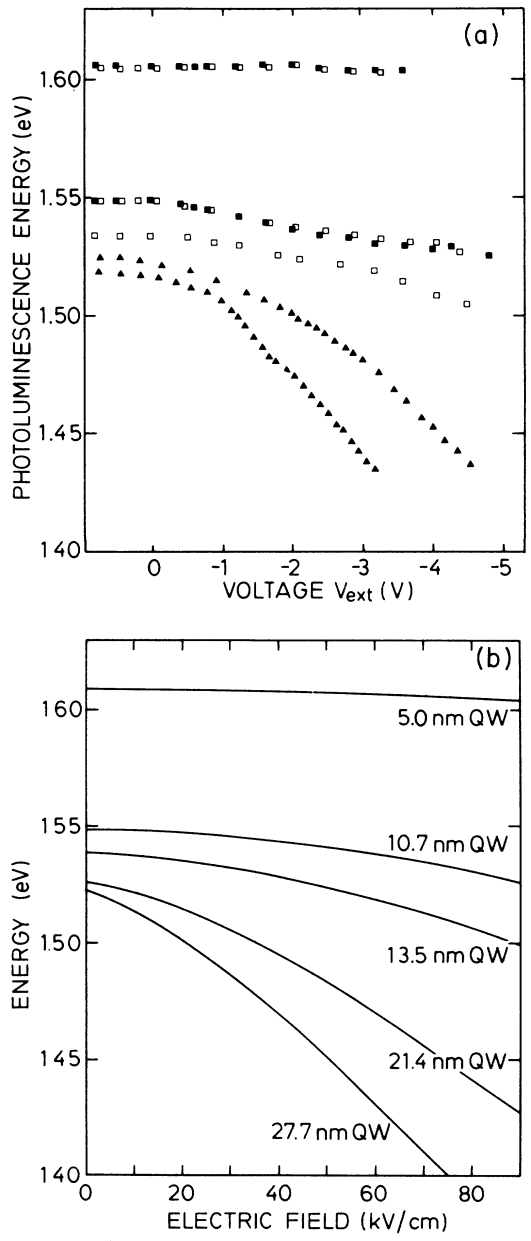

FIG. 2. (a) Photoluminescence peak energy as a function of external voltage V_{ext}. Open squares, solid triangles, and solid squares denote experimental points for three different excitation intensities of 1×10^{11}, 5×10^{11}, and 5×10^{12} photons/cm^2 per pulse, respectively. (b) Calculated excitonic energy for a finite quantum well exposed to an electric field perpendicular to the layers.

A simple consideration even allows us to determine the internal electric field F_{int} from the luminescence shift if the same external electric field is applied across two QW's of different width L_z. The transition energy E_{trans} as measured by luminescence is

$$E_{trans}=E_{well}+(E_g-eF_{int}L_z)\ , \tag{1}$$

where E_{trans} is separated into two contributions. (i) The energy E_{well} contains the sum of the confinement energies in the well (electrons E_e and holes E_h) determined from the bottom of each well, $E_{well}=E_e+E_h$ (see inset of Fig. 3). (ii) While the second part is the gap energy E_g of bulk GaAs reduced by the electrostatic potential $F_{int}L_z$ in the well times the elementary charge e. For high electric fields and reasonably broad QW's, the energy E_{well} of the $N=1$ level is exclusively determined by a triangular well (see inset of Fig. 3), i.e., no longer the width of the GaAs layer but the shape of the triangular potential determines E_{well}. Thus the energy E_{well} is independent of the layer thickness and only determined by the strength of the electric field. This is confirmed by our observations depicted in Fig. 3, where we plotted E_{well} (solid lines) as determined from our theoretical calculations versus layer thickness. At a field strength ≥ 60 kV/cm E_{well} becomes

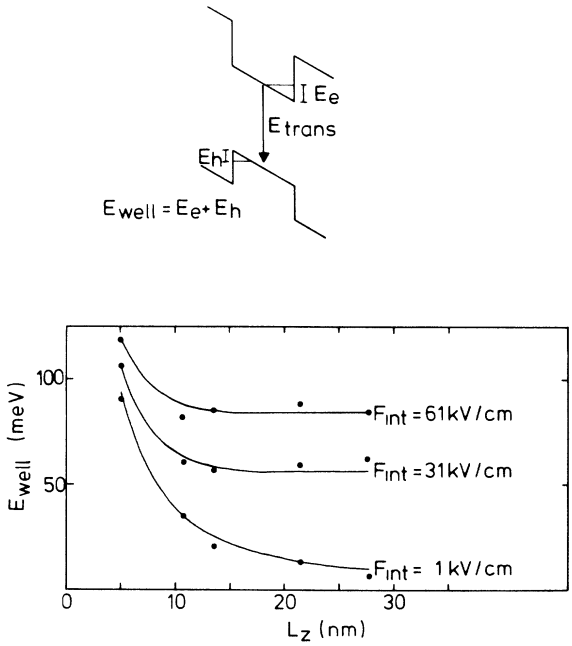

FIG. 3. The sum of the confinement energy of electrons and holes versus well thickness for three different electric fields as calculated in the model of the finite QW. The solid points denote the experimental values, as received by Eq. (1) from the photoluminescence spectra. The insert schematically demonstrates the meaning of the transition energy E_{trans} and the particle energies in the wells (electrons, E_e and holes, E_h) in an electric field where the particle energy is determined by a triangular well.

independent of the field at QW thicknesses ≥ 10 nm. The transition energy E_{trans} for different QW's in this case is only a function of $F_{\text{int}}L_z$, which is a simple geometric factor. Thus two QW's of different L_z in an identical electric field yield the possibility to determine the internal electric field via the transition energy given by Eq. (1). Subtracting two transition energies for two different QW's yields

$$F_{\text{int}} = \frac{e(L_{z2} - L_{z1})}{E_{\text{trans1}} - E_{\text{trans2}}} . \tag{2a}$$

Using Eq. (2a) for the 10.7- and 21.4-nm wells (sample no. 1) as well as the 13.5- and 27.7-nm wells (sample no. 2) at the highest possible fields we get the correspondent expression for the applied external voltage and the internal electric field:

$$1V_{\text{ext}} \hat{=} 15 \text{ kV/cm} . \tag{2b}$$

Taking this relation to determine E_{well} by means of Eq. (1) from our experimental data, one gets the experimental values (dots) in Fig. 3 giving confidence in our simple approximation.

The estimation of the *external* field strength as calculated from the applied voltage and the thickness of the depletion layer leads to values, which must be reduced by a factor of ≈ 2 to get agreement to the *internal* electric field. This discrepancy is not completely understood but might be attributed to screening of the field by charge carriers.

Results of the time-resolved measurements for the QW's of sample no. 1 with barrier thicknesses of 24 nm are summarized in Fig. 4. Lifetimes τ_0 at zero electric field ($V_{\text{ext}} = 0.9$ V) are shorter for thinner QW's due to carrier confinement which leads to enhanced recombination.[31,32] Decreasing the voltage V_{ext} yields a strong increase in photoluminescence lifetime by more than a factor of 100 for the thicker well, whereas no significant change is observed for the 5-nm QW for voltages down to -3 V.

Comparison of the experimental results with theoretical curves again gives good agreement, as shown by the dotted lines in Fig. 4 for sample no. 1. Here, the same model of a finite well as used for the evaluation of the energy shift in an electric field [see curves in Fig. 2(b)] has been applied under the assumption that the luminescence lifetime is given by the radiative recombination lifetime τ_r. In the one-particle picture

$$\tau_r = \tau_0 / |M_{\text{cv}}|^2 , \tag{3}$$

where M_{cv} is the overlap integral of the electron and hole wave functions, and τ_0 is the lifetime under flat-band condition.[33]

IV. FIELD IONIZATION

The strong decrease of the lifetime for the 5-nm– and 21.4-nm–thick QW's, however, as found for fields higher than those indicated by the arrows in Fig. 4 cannot by explained by the theoretical model of the QCSE, which implicitly neglects the influence of the field to the barrier

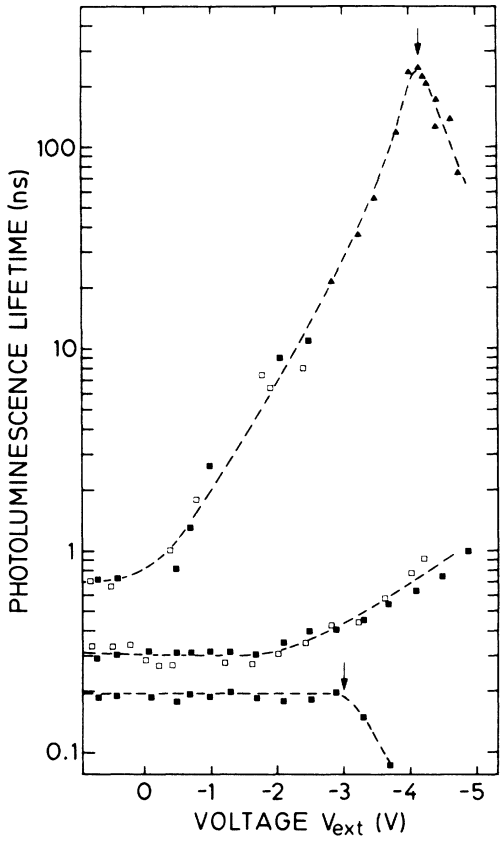

FIG. 4. Photoluminescence lifetime vs external voltage V_{ext} for the QW's in sample no. 1 ($L_z = 5$, 10.7, and 21.4 nm) with a barrier thickness $w_B = 24$ nm. For a description of the triangles and squares see Fig. 2(a). Dashed lines are a guide to the eye.

thickness. Although confined in the well by the barriers, the walls only inhibit separation, i.e., exciton ionization if the individual electrons and holes do not tunnel rapidly enough through the potential barriers, which strongly depends on the barrier thickness and the field. The actual shape of the potential, and thus the barrier thickness for the carriers within the well, is a superposition of the band scheme and the applied electric field. If the height of the potential barrier is comparable to the applied electric potential, the shape of the barrier becomes triangular and the change of the barrier thickness is appreciable. In this regime the decrease of the photoluminescence lifetime is due to the tunneling of carriers through the barriers (Fowler-Nordheim tunneling). Tunneling becomes dominant, leading to an increase of the photocurrent and competes with the carrier recombination in the well. Because of the competitive character of the tunneling out of QW's and the recombination within the QW's the final shape of the photoluminescence lifetime is determined by the rates of these two processes.

A. Tunneling and photoluminescence lifetime

A quantitative understanding of the measured photoluminescence lifetime in high electric fields has to incorporate the carrier separation within the well, as well as the

tunneling contribution through the barriers, which ultimately dominates the optical and electrical properties in the high-field limit. The strength of tunneling can be obtained accurately by evaluating the rate of tunneling of an individual particle in the model of the quasiclassical or Wentzel-Kramers-Brillouin (WKB) approximation.[34,35] The tunneling time τ_t for electrons is thus given by

$$\tau_t = \tau_p \exp\left[2\int_{z_0}^{z}\{2(m_e/\hbar^2)[eV(z)-E_e]\}^{1/2}dz\right], \quad (4)$$

where the exponential expression describes the relative changes of the tunneling time with the electric field. (The tunneling probability for heavy holes is smaller by several orders of magnitude.) The effective electron mass m_e has a value of $0.0916m_0$ in the barrier,[9] $V(z)$ is the potential for the electrons in the z direction of the barriers (perpendicular to the layers) including the potential of the electric field, E_e is the electron energy in the well (as calculated in the model of the finite QW), and $\hbar$ is the Planck constant divided by 2π. Integration is carried out over the actual barrier thickness w_A determined by

$$z - z_0 = w_A = \frac{eV_0 - E_e}{F} \quad \text{for } w_A < w_B , \quad (5a)$$

where w_B is the barrier thickness equivalent to the $Al_xGa_{1-x}As$ layer. For values of w_A which exceed the barrier thickness w_B

$$z - z_0 = w_B \quad \text{for } w_A \geq w_B . \quad (5b)$$

V_0 is the potential barrier height at zero electric field or the band-gap discontinuity in the conduction band.

In order to obtain absolute values for the tunneling time the exponential in expression (4) is multiplied with the cycle time τ_p, which is deduced by a simple classical consideration and represents the oscillation time of a classical oscillator. The probability for a particle to leave the QW on one side, depends on reaching the wall (colliding with the wall), and the tunneling probability. Classically this collision time with one wall is given by the covered distance $2L_z$ divided by the velocity v of the particle: $\tau_p = 2L_z/v$. Expressed in terms of the particle energy we obtain

$$\tau_p = \hbar\pi/E_e . \quad (6)$$

Taking this expression, we get values of τ_p in the relevant region of 30–90 kV/cm between $(3-6)\times10^{-14}$ s for QW's between 10 and 30 nm, while the 5-nm QW has values of $(2.3-2.6)\times10^{-14}$ s.

Applying our simple WKB model to the 9.5-nm QW as used for the tunneling resonance calculations of energy levels by Miller *et al.*,[9] we obtain good agreement of our theoretical curve with that in Fig. 9 of Ref. 9. This confirms the applicability of our model. Theoretical curves for the tunneling time τ_t of the QW's used in our experiments with a barrier thickness w_B of 24 nm (sample no. 1) are shown by the dashed lines in Fig. 5. Comparable tunneling rates and thus times are found for the two QW's with a width of 10.7 and 21.4 nm, which results from their rather similar energies in the wells due to the triangular shape of the wells at electric fields above 60 kV/cm (see Fig. 3). The particles in the 5-nm QW have still higher tunneling rates and therefore smaller lifetimes at the same electric field strength. Here the strong decrease of τ_t is caused by two effects: First a decrease of the actual barrier thickness due to the higher confinement energy of the carriers and second the cycle time τ_p is significantly reduced.

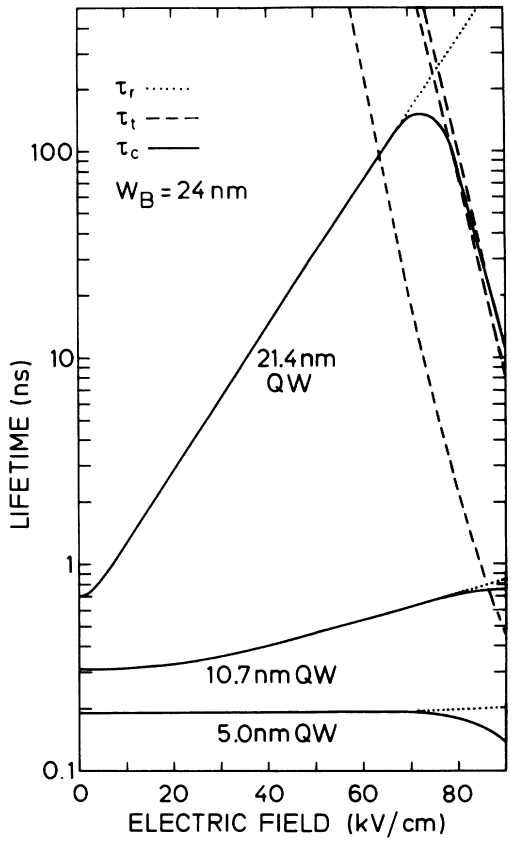

FIG. 5. Calculated radiative lifetime τ_r (dotted line), tunneling time τ_t (dashed line), and carrier lifetime τ_c (solid line) as function of electric-field strength for sample no. 1 with a barrier thickness $w_B = 24$ nm.

According to the Mathiessen rule the photoluminescence lifetime τ_c in the presence of a tunneling rate $1/\tau_t$ is then given by

$$1/\tau_c = 1/\tau_r + 1/\tau_t . \quad (7)$$

The solid lines in Fig. 5 describe τ_c as a function of the field strength. At high electric fields τ_t is smaller than τ_r and the tunneling rate of the carriers efficiently competes with the radiative recombination rate. The effectivity of the rates are essential for the actual behavior of the total lifetime of a QW. Both rates are changing drastically for the broadest QW. The field, where tunneling efficiently competes with the radiative recombination, is expected to be within our experimentally accessible region. For the 10.7-nm QW, however, it is expected, that the radiative rate dominates within the whole measuring range. For

the thinnest QW again the tunneling rate is much higher and competes already at smaller fields with the constant radiative rate, leading to a decrease of the τ_c at ≈ 80 kV/cm.

A comparison of the theoretical results (Fig. 5) with the measured lifetimes (Fig. 4) due to relation (2b) again shows good agreement. In particular, the strong influence of the tunneling in the 5-nm and the 21.4-nm QW and the insensitivity of the 10.4-nm QW on tunneling are well described.

B. Influence of the barrier thickness w_B

In the regime of the QCSE, only the particle energy in the well and the barrier height have to be considered in order to evaluate the optical properties, whereas the barrier thickness has no influence. In contrast, in the regime of field ionization the barrier thickness strongly influences the tunneling time. Due to Eqs. (4) and (5a) the decrease of τ_t is caused by the decrease of the actual barrier thickness as well as the increase of the confinement energy.

In the preceding chapter the effects of field ionization have been mainly discussed in the range where $w_A < w_B$, i.e., the integration range and so the actual barrier thickness w_A is exclusively determined by the parameters electric field and electron energy within the well. In order to study the influence of a different barrier thickness, we therefore have to use QW's within a smaller barrier thickness w_B. Due to Eq. (5b) w_A has to exceed w_B which leads to a constant integration range of Eq. (4). An increase of w_B would bring no additional information.

Experimental results for QW's with QW widths comparable to those of sample no. 1 but smaller barrier thickness are obtained for sample no. 2, where the barrier thickness is reduced to $w_B = 14$ nm. This barrier thickness is such, that the integration range of Eq. (4) is constant up to electric fields of 90 kV/cm, i.e., within the measuring range. The data of sample no. 2 with $L_z = 27.7$ and 13.5 nm are shown in Fig. 6. Included are also the data of sample no. 1 with $w_B = 24$ nm and a QW width of $L_z = 21.4$ and 10.7 nm. The comparison of the two sets of data of samples with different barrier thicknesses demonstrates that the onset of field ionization shifts to smaller electric fields for the QW's with thinner barriers, confirming the prominent influence of the barrier thickness. Theoretical curves of the lifetime for the QW's of sample no. 2 are shown in Fig. 7. The pronounced increase of the lifetime due to QCSE is superceeded by the field ionization for both QW's at electric field strengths of 45 kV/cm and 80 kV/cm for the 27.7 nm and 13.5 nm QW, respectively. The tunneling time τ_t of the QW's is not significantly different due the triangular shape of the QW's in an electric field, which yields an E_e for both QW's with only a difference of 0.5–1.5 meV for the relevant electric fields (see Fig. 3). The distinct influence of the thinner barriers as seen in Fig. 6 and the onset of tunneling at smaller electric fields is well described by the theory in Fig. 7 on the basis of the relation (2b).

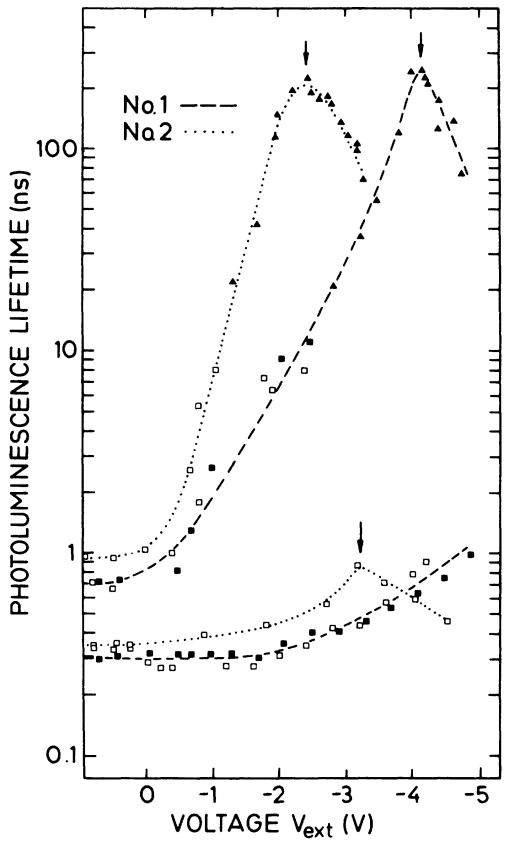

FIG. 6. Carrier lifetime as a function of external voltage V_{ext} for samples with different barrier thicknesses. The dashed line is a guide to the eye for QW's with 24-nm barrier layers, respectively, the dotted line for QW's with 14-nm–thick barriers. For a description of the triangles and squares see Fig. 2(a).

C. Photoluminescence quenching and tunneling current

The knowledge of the electric field dependence of the photoluminescence lifetime in QW's allows us to separate the regime of the QCSE and the regime of field ionization. Additional evidence and completion of the results from the lifetime behavior with respect to field ionization is given by comparing the recombination in the well via photoluminescence intensity and charge separation out of the well via tunneling current. The luminescence intensity versus the external voltage in Fig. 8 shows a relatively slight decrease by less than 40% in the range where the lifetime behavior is mainly influenced by the QCSE. However, in the range of field ionization, where the main recombination channel is tunneling through the barriers, the luminescence intensity drops over nearly two decades. Simultaneously the disappearance of the charge carries in luminescence gives rise to a tunneling current ΔI. These observations confirm our interpretation, that the decrease of lifetime is due to field ionization which is supported by the sharp concomitant decrease of the photoluminescence intensity as well as the strong increase of the tunneling current ΔI.

In the model for the determination of the total lifetime τ_c, we considered the two processes radiative recombina-

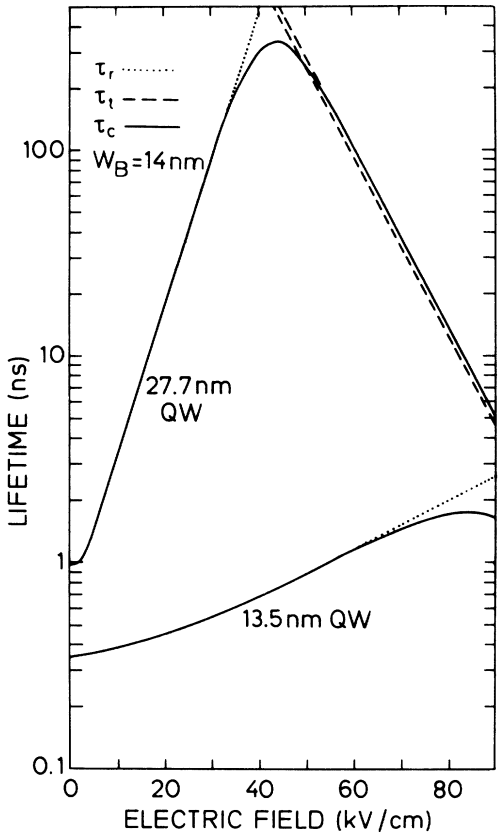

FIG. 7. Calculated radiative lifetime τ_r (dotted line), tunneling time τ_t (dashed line), and carrier lifetime τ_c (solid line) as function of electric-field strength for sample no. 2, with a barrier thickness $w_B = 14$ nm.

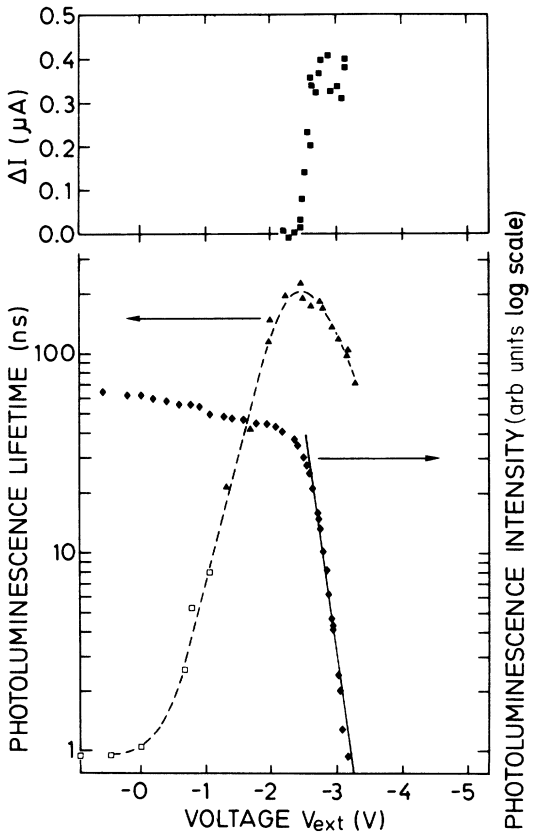

FIG. 8. Lower part: Photoluminescence lifetime (dashed guide line) and intensity (rhombs) vs V_{ext} together with the tunneling current of the 27.7-nm–thick QW (sample no. 2). The solid line represents an evaluation of the decrease of the luminescence intensity from lifetime measurements (see text). For a description of the triangles and squares see Fig. 2(a). Upper part: Tunneling current ΔI vs V_{ext}. ΔI results from subtracting the extrapolated photocurrent I_{photo} from the measured total current I_{total}: $\Delta I = I_{total} - I_{photo}$. I_{photo} is determined by extrapolating the current, measured in the range of the QCSE, into the range of field ionization. The dark current of 0.1 μA is constant in the measuring range.

tion and tunneling. The rates determined from these two processes yield a photoluminescence intensity P which is proportional to

$$P \sim \frac{1/\tau_r}{1/\tau_r + 1/\tau_t} . \tag{8}$$

As long as $\tau_t \gg \tau_r$, there is only radiative recombination valid for small electric fields and the luminescence intensity is expected to be constant, which is in relatively good agreement to the experimental results. The observed small decrease might be due to some background nonradiative transitions via imperfections and deep impurities. In the regime of field ionization where $\tau_t \ll \tau_r$, tunneling out of the well dominates. The expression (8) for the luminescence reduces to

$$P \sim \frac{1/\tau_r}{1/\tau_t} . \tag{9}$$

Thus, the luminescence intensity is proportional to the decreasing radiative rate $1/\tau_r$ divided by the increasing tunneling rate $1/\tau_t$ giving rise to a pronounced decrease of the intensity. By extrapolating the lifetime of the regime of the QCSE, which is equivalent to τ_r, we determine the decrease of the luminescence intensity from the lifetime measurements. The result is shown in Fig. 8 by the solid line which is in excellent agreement to the measurement.

V. CONCLUSION

In summary we have studied the electric-field-induced dynamics of 2D excitons in GaAs/$Al_xGa_{1-x}As$ QW's. We have elucidated the role of the QCSE and the corresponding spectral and temporal features for the low-field region, as well as carrier tunneling, i.e., excitonic field ionization in the high-field regime. Thus a consistent and

complete picture of the electric field related photoluminescence of excitons in QW's is obtained.

ACKNOWLEDGMENTS

The authors would like to thank E. O. Göbel, J. Kuhl, and H. J. Queisser for their encouraging and helpful discussions and for critical reading of the manuscript. We gratefully acknowledge the expert technical assistance of W. Heinz and K. Rother. Thanks are due to R. F. Kopf for assisting in the molecular beam epitaxy growth and to H. Oppolzer/Siemens for providing the TEM measurements.

---

*Present address: Fraunhofer-Institut für Angewandte Festkörperphysik, D-7800 Freiburg, FRG.

†Present address: Dr. J. Heidenhain GmbH, D-8225 Traunreut, FRG.

‡Present address: ASEA Brown Boveri Corporate Research, CH-5405 Baden-Dättwil, Switzerland.

[1]H.-J. Polland, L. Schultheis, J. Kuhl, E. O. Göbel, and C. W. Tu, Phys. Rev. Lett. **55**, 2610 (1985).

[2]L. Viña, R. T. Collins, E. E. Mendez, and W. I. Wang, Phys. Rev. B **33**, 5939 (1986).

[3]L. Viña, R. T. Collins, E. E. Mendez, W. I. Wang, L. L. Chang, and L. Esaki, Superlatt. Microstruct. **3**, 9 (1987).

[4]M. Yamanishi, Y. Usami, Y. Kan, and I. Suemune, Jpn. J. Appl. Phys. **24**, L586 (1985).

[5]*Proceedings of the 18th International Conference on the Physics of Semiconductors, Stockholm, 1986,* edited by O. Engström (World Scientific, Singapore, 1987), p. 533.

[6]L. Schultheis, K. Köhler, and C. W. Tu, Phys. Rev. B **36**, 6609 (1987).

[7]L. Schultheis, A. Honold, J. Kuhl, K. Köhler, and C. W. Tu, Phys. Rev. B **34**, 9027 (1986).

[8]D. A. B. Miller, D. S. Chemla, T. C. Damen, A. C. Gossard, T. H. Wood, and C. A. Burrus, Phys. Rev. Lett. **53**, 2173 (1985).

[9]D. A. B. Miller, D. S. Chemla, T. C. Damen, A. C. Gossard, T. H. Wood, and C. A. Burrus, Phys. Rev. B **32**, 1043 (1985).

[10]J. A. Kash, E. E. Mendez, and H. Morkoc, Appl. Phys. Lett. **46**, 173 (1985).

[11]E. J. Austin and M. Jaros, Appl. Phys. Lett. **47**, 274 (1985).

[12]E. E. Mendez, G. Bastard, L. L. Chang, L. Esaki, H. Morkoc, and R. Fischer, Physica **117B&118B**, 711 (1983).

[13]H. Iwamura, T. Saku, and H. Okamoto, Jpn. J. Appl. Phys. **24**, 104 (1985).

[14]C. Alibert, S. Gaillard, J. A. Brum, G. Bastard, P. Frijlink, and M. Erman, Solid State Commun. **53**, 457 (1985).

[15]J. A. Brum, and G. Bastard, Phys. Rev. B **31**, 3893 (1985).

[16]P. W. Yu, D. C. Reynolds, K. K. Bajaj, C. W. Litton, W. T. Masselink, R. Fischer, and H. Morkoc, J. Vac. Sci. Technol. B **3**, 624 (1985).

[17]E. J. Austin and M. Jaros, Phys. Rev. B **31**, 5569 (1985).

[18]Y. Horikoshi, A. Fischer, and K. Ploog, Phys. Rev. B **31**, 7859 (1985).

[19]Y. Kan, M. Yamanishi, I. Suemune, H. Yamamoto, and T. Yao, Jpn. J. Appl. Phys. **24**, 589 (1985).

[20]K. Yamanaka, T. Fukunaga, N. Tsukada, K. L. I. Kobayashi, and M. Ishii, Appl. Phys. Lett. **48**, 840 (1986).

[21]Y. Masumoto, S. Tarucha, and H. Okamoto, Phys. Rev. B **33**, 5961 (1986).

[22]E. E. Mendez, E. Calleja, C. E. T. Goncalves da Silva, L. L. Chang, and W. I. Wang, Phys. Rev. B **33**, 7368 (1986).

[23]F. Borondo and J. Sánchez-Dehesa, Phys. Rev. B **33**, 8758 (1986).

[24]M. Matsuura and T. Kamizato, Phys. Rev. B **33**, 8385 (1986).

[25]D. A. B. Miller, J. S. Weiner, and D. S. Chemla, IEEE J. Quantum Electron. **QE-22**, 1816 (1986).

[26]E. O. Göbel, in *Excitons in Confined Systems, Rome, 1987,* Vol. 25 of *Springer Proceedings in Physics,* edited by R. Del Sole, A. D'Andrea, and A. Lapiccirella (Springer, Berlin, 1988), p. 204.

[27]H.-J. Polland, Y. Horikoshi, E. O. Göbel, J. Kuhl, and K. Ploog, Surf. Sci. **174**, 278 (1986).

[28]H.-J. Polland, Y. Horikoshi, E. O. Göbel, J. Kuhl, and K. Ploog, Physica **134B**, 412 (1985).

[29]L. Schultheis, K. Köhler, and C. W. Tu, in Ref. 26, p. 110.

[30]R. L. Greene, K. K. Bajaj, and D. E. Phelps, Phys. Rev. B **29**, 1807 (1984).

[31]E. O. Göbel, H. Jung, J. Kuhl, and K. Ploog, Phys. Rev. Lett. **51**, 1588 (1983).

[32]R. Höger, E. O. Göbel, J. Kuhl, K. Ploog, and G. Weimann, *Proceedings of the 17th International Conference on the Physics of Semiconductors, San Francisco, 1984,* edited by J. D. Chadi and W. A. Harrison (Springer, New York, 1985), p. 175.

[33]G. Bastard, E. E. Mendez, L. L. Chang, and L. Esaki, Phys. Rev. B **28**, 3241 (1983).

[34]L. I. Schiff, *Quantum Mechanics* (McGraw-Hill, Tokyo, 1986).

[35]L. D. Landau and E. M. Lifshitz, *Quantum Mechanics–Nonrelativistic Theory* (Pergamon, New York, 1981).